Hindawi Publishing Corporation
Journal of Engineering
Volume 2016, Article ID 2308560, 9 pages
http://dx.doi.org/10.1155/2016/2308560

Research Article

Sorption Profile of Phosphorus Ions onto ZnO Nanorods Synthesized via Sonic Technique

M. F. Elkady,[1,2] H. Shokry Hassan,[3] and Eslam Salama[4]

[1]*Chemical and Petrochemical Engineering Department, Egypt-Japan University of Science and Technology, New Borg El-Arab City, P.O. Box 21934, Alexandria, Egypt*
[2]*Fabrication Technology Research Department, Advanced Technology and New Materials Research Institute (ATNMRI), City of Scientific Research and Technological Applications, New Borg El-Arab City, P.O. Box 21934, Alexandria, Egypt*
[3]*Electronic Materials Research Department, Advanced Technology and New Materials Research Institute (ATNMRI), City of Scientific Research and Technological Applications, New Borg El-Arab City, P.O. Box 21934, Alexandria, Egypt*
[4]*Environment and Natural Materials Research Institute (ENMRI), City of Scientific Research and Technological Applications, New Borg El-Arab City, Alexandria, Egypt*

Correspondence should be addressed to M. F. Elkady; marwa.f.elkady@gmail.com

Received 30 November 2015; Accepted 17 March 2016

Academic Editor: Jong M. Park

High surface area zinc oxide material in nanorod morphological structure was synthesized using an ultrasonic technique in the presence of polyvinyl pyrrolidone as stabilizing agent. The crystallite, morphology, and surface area of the prepared white powder material were identified using XRD, SEM, and BET techniques, respectively. X-ray analysis confirms the high purity of synthesized ZnO. The evaluated specific surface area of prepared ZnO was 16.7 m^2/g; this value guarantees high efficiency for water purification. The feasibility of synthesized ZnO nanorods for phosphorus sorption from aqueous solution was established using batch technique. Nano-zinc oxide exhibits high efficiency for phosphorus removal; the equilibrium state was recorded within 90 minutes. The most effective hydrogen ion concentration of the polluted solution was recorded at pH = 1 for phosphorus decontamination. The equilibrium of phosphorus sorption onto ZnO nanorods was well explained using both Langmuir and Temkin isotherm models. The calculated maximum monolayer sorption capacity was 89 mg/g according to Langmuir isotherm at 27°C. In order to explain the phosphorus sorption mechanism onto the prepared ZnO nanorods, three simplified kinetic models of pseudo-first order, pseudo-second order, and intraparticle diffusion rate models were tested. Kinetics was well fitted by pseudo-second order kinetic model with a contribution of intraparticle diffusion.

1. Introduction

Zinc oxide (ZnO) is a polar inorganic crystalline material with many applications due to its unique combination of interesting properties such as nontoxicity, good electrical, optical, and piezoelectric behavior, stability in a hydrogen plasma atmosphere, and low price. Nanostructured ZnO crystals can be synthesized in solution or gaseous phases [1]. In material science, zinc oxide is classified as a semiconductor in groups II–VI, whose covalence is on the boundary between ionic and covalent semiconductors. These properties give ZnO the electrical amphoteric property as n-type semiconductor in most preparation procedures [2]. Nano-ZnO has novel characteristic properties which provide the opportunity of the material to be utilized in many applications including wastewater treatment, antimicrobial agent, and electronics [3]. The increase in surface area of nanoscale ZnO compared to bulk material has the potential to improve the efficiency of the material function [4]. Accordingly, nano-ZnO attracted significant attention as an adsorbent material for cations and anions pollutants from polluted water [5]. Recently, many techniques were developed to synthesize nanostructured zinc oxide including vapor phase growth, vapor-liquid-solid process, soft chemical method, electrophoretic deposition, sol-gel process, and homogeneous precipitation [6]. The sonochemical technology was established as practical technique

for production novel materials with interesting properties. This technology is based on acoustic cavitations resulting from the continuous formation, growth, and implosive collapse of bubbles in a liquid [6]. This preparation technique has been used for the synthesis of many kinds of nanomaterials. With respect to ZnO, this technology was adapted to fabricate ZnO in various nanomorphological structures [7].

Phosphate represents an essential nutrient for the growth of photosynthetic cyanobacteria and algae [8]. Phosphorus is considered the limiting water-quality constituent responsible for accelerated eutrophication in water bodies [9]. The main resources of P that enter water body either rivers or lakes were from household, agricultural, or industrial wastes [10]. In wastewater, P is in the forms of phosphate ($H_2PO_4^-$, HPO_4^{2-}, and PO_4^{3-}), organic phosphate, and polyphosphate [11]. The dissolved phosphate is easily absorbed by algae while the polyphosphates and organic phosphate could be hydrolyzed into the phosphate forms [12]. A wide array of technologies is being developed to reduce point and nonpoint P pollution using multiple combinations of different processes such as chemical reduction, biological, precipitation, and adsorption [13, 14]. Adsorption process is collecting soluble substances from solution to a suitable interface [15] and it is an easy method and finding a cheap sorbent with high capacity of removal represents very important aspect. To date, remarkable progress has been made on the synthesis of high sorption nanoparticles specifically tailored for environmental remediation. The small feature size of nanomaterials greatly influences their active surface areas which lead to the increase of adsorption capacity of the remediation agent compared to bulk materials. Thus, zinc oxide will be synthesized in nanorod morphological structure to be characterized with high active surface area available for sorption process. The nanorod fabrication of ZnO will be accomplished with the assistance of sonication technique in the presence of high molecular weight stabilizing agent of polyvinyl pyrrolidone. The physicochemical properties of prepared nanomaterial will be explored using different characterization techniques. The feasibility of the prepared ZnO nanorods toward phosphorus decontamination was examined using batch technique. The influence of variation of the processing parameters of phosphorus removal onto ZnO decontamination efficiency was explored. Finally, the experimental results of phosphorus removal process were modeled using different equilibrium and kinetics equation models to describe the nature of the decontamination process onto the prepared ZnO nanorods.

2. Experimental

2.1. Preparation of ZnO Nanopowdered Material. The ZnO nanopowders were prepared via ultrasonic technique. 0.3 M aqueous solution of $Zn(NO_3)_2$ was prepared at room temperature in a glass beaker under magnetic stirring by adding zinc nitrate into 250 mL of distilled water. 0.03 M polyvinyl pyrrolidone solution (molecular weight = 30,000) was prepared in the presence of 1 mol/L NH_4OH. This solution mixture was dispersed in zinc nitrate solution. The solution mixture was sonicated using direct sonication probe ultrasonic homogenizer (Sonics Vibra-Cell VCX 500, USA). Ultrasonic energy was applied in continuous sonication mode, the power intensity was fixed at 40% amplitude, and the sonication temperature was fixed at 70°C. After finishing the sonication period of 1 hour, a white precipitate of nanopowdered ZnO appeared. The resultant powder material was separated by centrifugation. The white precipitate was washed several times with alcohol and distilled water to remove any residual salts or stabilizing agent and was dried at 60°C.

2.2. Characterization of Prepared ZnO Nanopowdered Material. In order to determine the crystalline, morphological structure and specific surface area of prepared ZnO powder material, it was analyzed using different physicochemical techniques. X-ray powder diffraction (XRD) measurements were performed using Shimadzu 7000 diffractometer with monochromatized Cukα radiation to identify the crystalline structure of prepared ZnO. The material morphology was characterized using both Scanning Electron Microscopes (JEOL JSM 6360LA, Japan) with gold coating and Transmission Electron Microscope TEM (JEOL JEM-1230, Japan) of ethanol suspended powder material. Following the classic Brunauer-Emmett-Teller method, the specific surface area of prepared ZnO was determined using surface area analyzer (Belsorp II mini, BEL Japan Inc.). Adsorption of pure nitrogen by specific weight of powdered ZnO was performed under relative pressures range from 0.05 to 0.3. The specific surface area of the samples was calculated using quantities of adsorbed N_2.

2.3. Assessment of Prepared ZnO Nanopowder for Phosphorus Decontamination. The adsorption capacity of prepared ZnO for phosphorus decontamination was determined using batch technique. Firstly, potassium phosphate solution contains 1000 mg PO_4/L prepared as synthetic waste solution for further dilutions. A specific amount from the prepared nano-ZnO was mixed with 25 mL from synthetic waste solutions at different phosphorus concentrations for a definite mixing time. The mixing process takes place at caped polypropylene plastic vials (50 mL) using rotated end-over-end in a custom-made shake at 40 rpm. The periodical samples were withdrawn at different specific intervals to measure the reaming phosphorus concentrations using the ascorbic acid-molybdate blue method [16]. This method depends on the formation of phosphomolybdic acid during the reaction between orthophosphate and molybdate. Ascorbic acid reduces phosphomolybdic to form a blue complex. The color was measured at a wavelength of 885 nm with a spectrophotometer. Based on initial (C_0) and final measured concentration (C) of each sample, the percentage of phosphorus onto nano-ZnO will be estimated.

A series of batch studies was carried out to examine the effect of variation phosphorus removal parameters on the decontamination process onto prepared nano-ZnO. The effects of contact time (0–240 minutes), initial phosphorus concentration (1, 10, 50, 100, and 200 ppm), material dosage (4–40 g/L), and solution pH (1–11) were optimized.

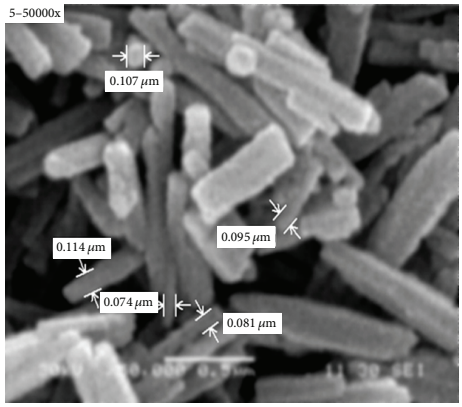

Figure 1: SEM micrograph of prepared ZnO nanorods.

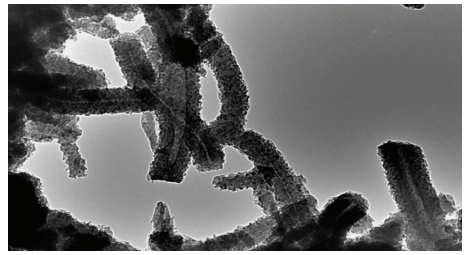

Figure 2: TEM micrograph of prepared ZnO nanorods.

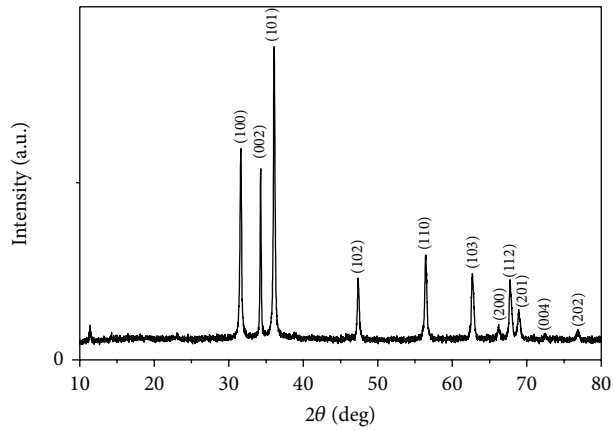

Figure 3: XRD patterns for ZnO nanopowders.

2.4. Equilibrium and Kinetic Modeling of Phosphorus Decontamination Process onto Prepared ZnO Nanorods. Equilibrium and kinetic modeling is very important for establishing an adsorption system and provides information on the capacity of the adsorbent or the amount required for removing a unit mass of pollutant under the designated conditions. So, the experimental data that resulted from phosphorus decontamination onto the prepared nano-ZnO were modeled using Langmuir, Freundlich, and Temkin equilibrium isotherm adsorption models. As an attempt to explain the adsorption mechanism of phosphorus ions onto the prepared nano-ZnO, pseudo first-order equation, second-order, and intraparticle diffusion equations were applied.

3. Results and Discussion

3.1. Characterizations of Prepared ZnO Nanopowdered Material. Morphology and structure of prepared ZnO were explored by Scanning Electron Microscopy (SEM). Figure 1 investigates the formation of a great quantity from straight long rods mixed with small amounts of shorter rods. The average diameter of prepared ZnO nanorods is 100 nm and the calculated average aspect ratio of the prepared nanorods was 6. Accordingly, this micrograph of ZnO nanopowder indicates that ultrasonic technique in presence of PVP as a stabilizing agent has the ability to fabricate ZnO in nanorod morphological structure. This result may be owed to the role of PVP presence at the preparation media with the assistance of sonic waves. It was suggested that the presence of high molecular weight capping molecule (such as PVP) in the reaction media can alter the surface energy of crystallographic surfaces, in order to promote the anisotropic growth of the nanocrystals [17, 18]. In this regard, the high molecular weight PVP may be adsorbed on the ZnO crystal nuclei and it helps the particles to be arranged and to grow in the nanorod morphology. In order to confirm this suggested ZnO formation mechanism for nanorod production, TEM image was investigated in Figure 2. It was evident from this figure that the prepared matrix was produced in homogeneous nanorod morphological structure. This nanorod morphology affords the prepared ZnO high surface value that measured using BET method as 16.7 m^2/g.

XRD pattern of the direct sonochemically synthesized ZnO nanorods was indicated in Figure 3. It was established that the as-synthesized ZnO nanopowders produced diffraction patterns that are well indexed as crystalline hexagonal phase wurtzite structure which can be indexed with the zinc oxide wurtzite phase (JCPDS Card number 01-089-1397). No peaks attribute to possible impurities is observed. The sharp diffraction peaks signify that the as-prepared ZnO nanorods have high degree of crystallinity [19].

3.2. Assessment of Prepared ZnO Nanopowder for Phosphorus Decontamination

3.2.1. Effect of Solution pH on Phosphorus Removal Process. The solution pH represents an essential parameter in the adsorption process. This parameter not only affects the behavior of adsorbate ions in the solution but also affects the adsorbent material itself. Figure 4 demonstrates the change in phosphorus removal efficiency when pH changed from 1 to 10 with initial phosphorus concentration of 10 mg/L. It was indicated that the high adsorption efficiency was recorded within pH range 1 to pH range 5, with almost 99% phosphorus adsorption efficiency. This efficiency was declined rapidly at solution pH value of 11 to about 30% from its initial value. Accordingly, the most effective pH value for phosphorus removal was recorded within range of 1–6. The decline in the phosphorus adsorption after this pH range may be due to the

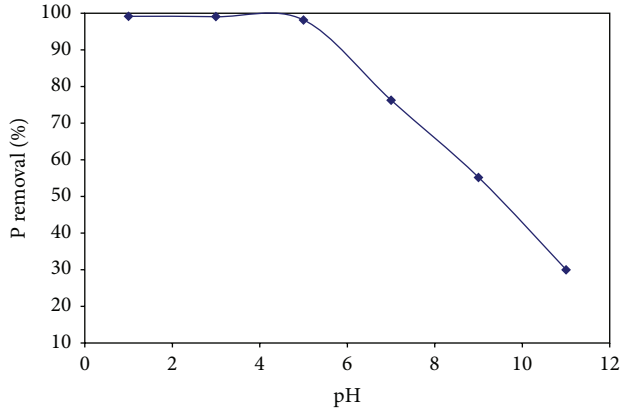

Figure 4: Effect of solution pH on phosphorus removal process onto ZnO nanorods.

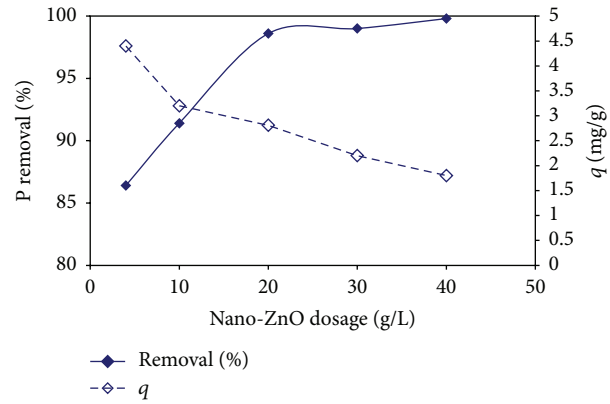

Figure 5: Effect of ZnO nanorods dosage on phosphorus removal process.

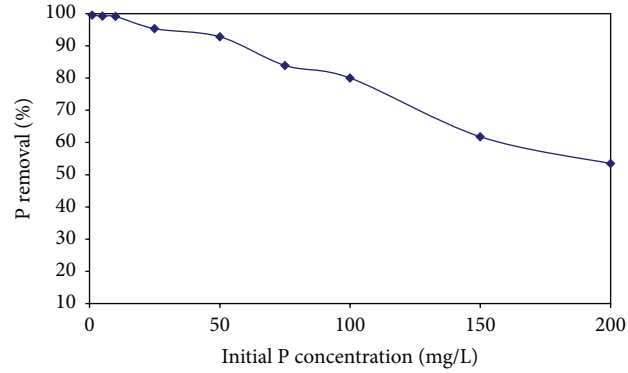

Figure 6: Effect of initial phosphorus concentration on sorption process onto ZnO nanorods.

fact that, with the increase in pH, OH^- concentration in the solution increases, which competes with phosphate anions ($H_2PO_4^-$, HPO_4^{-2}, and PO_4^{-3}) onto the ZnO adsorption sites [20]. On the other hand, regarding the amphoteric properties of nano-ZnO, the surface of the material may subject to protonation/deprotonation relying heavily on the solution pH. This behavior is known as acid-base property of the metal oxide surfaces that have considerable implications on their adsorption activity. It is well known that the zero-point charge for ZnO is 9.8 which is known as isoelectrical point (IEP) of ZnO, and, below this value, ZnO surface is positively charged by means of adsorbed H^+ ions [21]. So, the net surface charge of ZnO is positive at pH < 6, which is beneficial for adsorbing the phosphate anions [22]. This explains the observations of high P uptake in acidic condition (pH < 6). An increase of solution pH resulted in a buildup of negative charges on both nano-ZnO and adsorbate leading to an enhanced electric repulsion between the two phases. Based on these results, the suggested phosphorus adsorption mechanism onto the prepared ZnO nanorods may be expressed as in the following equation:

$$\text{=Zn-OH} + HPO_4^{-2} \longleftrightarrow \text{=Zn-}PO_4^{-2} + H_2O \quad (1)$$

Consequently, a sharp decreasing P adsorption was recorded at high solution pH. So, the presence of strong hydroxyl ions in the treatment solution restricts the approach of adsorption phosphate anions as a consequence of repulsive force.

3.2.2. Effect of ZnO Dosage on Phosphorus Removal Process. The adsorbent dose in solution will have an effect on both the percentage of adsorbate decontamination and the material adsorption capacity. The variation on both percentage of phosphorus removal and nano-ZnO capacity at selected contact time of 90 min keeping initial solute concentration at 10 ppm and solution pH at 5 was explored in Figure 5. As expected, the removal of P increases from 86.4% to 99.8% as ZnO dosage increased from 4 to 40 g/L. This can be due to the improvement at the available adsorption active sites for binding of P ions with increasing adsorbent dosage [23]. Moreover, it was indicated that above the dosage of 20 g/L from ZnO, there is no significant change in the percentage removal of phosphorus. This behavior may be attributed to the saturation of adsorption sites onto the prepared material. The saturation of the active sites may also be due to the overlapping of active sites at higher dosage as well as the decrease in the effective surface area resulting in the accumulation of material particles. So, 20 g/L is considered as the optimum nano-ZnO dosage for P decontamination. In spite of the increment in the P adsorption with material dosage, the material adsorption capacity was declined. This phenomenon is regarding the presence of fixed amount of P ions bound to the adsorbent and the amount of free ions remains constant at the solution even with further addition of the material dosage.

3.2.3. Effect of Initial Phosphorus Concentration on Phosphorus Removal Process. Figure 6 illustrates that the adsorption of P obviously depended on its initial concentration using the predetermined material optimum dosage 20 mg/L at solution pH of 5. It was observed that, for low initial concentrations of phosphorus (1–50 mg/L), the percent of decontamination onto ZnO nanorods was comparatively greater than that of the higher initial phosphorus concentrations (>50 mg/L). The percentage of P adsorption onto the prepared nano-ZnO is almost greater than 90% for solution phosphorus

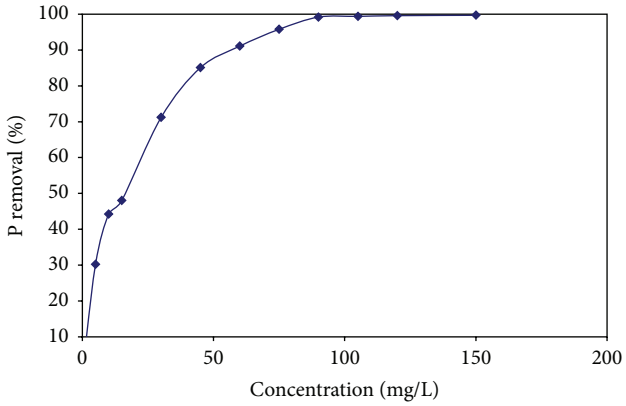

Figure 7: Effect of contact time on phosphorus removal process onto ZnO nanorods.

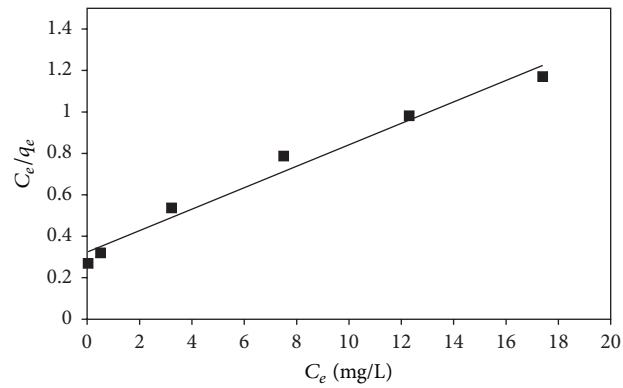

Figure 8: Langmuir equilibrium isotherm model for phosphorus ions sorption onto ZnO nanorods.

concentration less than 50 ppm. As the initial concentration improved above 50 ppm, the adsorption percentage declines till it reached 53% for the highest studied concentration of 200 ppm. The availability of adsorptive sites at ZnO nanorods is a possible explanation for this phenomenon [24] where the specific weight of nano-ZnO has a limited number of active sites, which become saturated with phosphorus ions at a certain concentration.

3.2.4. Effect of Contact Time on Phosphorus Removal Process. The change of phosphorus concentration as a function of time onto 0.1 mg/L from the prepared ZnO nanorods was studied using 10 ppm initial P concentration at a solution pH of 5. Figure 7 reveals that the rate of percent P removal is higher at the beginning. That is probably due to larger surface area of ZnO that was fabricated in nanorod morphological structure, which is available at the beginning for the adsorption of ions. As the surface adsorption sites become exhausted, the uptake rate is controlled by the rate at which the adsorbate is transported from the exterior to the interior sites of the adsorbent particles. It was indicated that the efficiency increased rapidly in 30 minutes after starting shaking and began slowly until it reached saturation. Removal efficiency of about more than 70% for dissolved phosphorus can be achieved after 30 minutes. This phosphorus removal efficiency onto the prepared matrix was reaching its completeness of 99% after 90 minutes. This result indicated the high ability of ZnO nanorods for phosphate adsorption at a short contact time to reach equilibrium. According to the results, system reached equilibrium within around 90 minutes; additional time could not cause any significant P reduction. So, the equilibrium time of adsorption P ions onto the prepared ZnO nanorods was recorded at 90 mins (full saturation of ZnO as a sorbent material). So, the prepared ZnO nanorods represent an efficient and time saving phosphorous decontamination process compared with other previously prepared matrices such as magnetic particles [25] where the prepared ZnO nanorods recorded 99% phosphorus removal within 90 minutes for the initial phosphorus ions concentration of 10 ppm, compared with 90% phosphorus removal within 120 minutes using magnetic particle for the same initial phosphorus ions concentration [25].

3.3. Equilibrium Isotherm Modeling of Phosphorus Sorption Process. The experimental data of phosphorus adsorption process onto ZnO nanorods were applied to three equilibrium isotherm adsorption models. These equilibrium models were performed to investigate the coverage or adsorption of P molecules on ZnO solid surface at a fixed temperature as an attempt to describe the behavior of the adsorption process.

3.3.1. Langmuir Model. It is considered as a commonly applied model of adsorption on a completed homogenous surface with negligible interaction between adsorbed molecules. This model assumes uniform adsorption energies onto the surface and maximum adsorption depends on the saturation level of monolayer. This model could be represented with the following linear equation [24]:

$$\frac{C_e}{q_e} = \left(\frac{1}{q_m K}\right) + \left(\frac{C_e}{q_m}\right), \quad (2)$$

where q_e is the amount of solute adsorbed per unit weight of sorbent (ZnO) at equilibrium (mg/g), C_e is the equilibrium concentration of P in the bulk solution (mg/L), and q_m is the monolayer capacity [25].

The plot of C_e/q_e versus C_e (Figure 8) indicates a straight line with high value of the correlation coefficient (R^2 = 0.9769) for the linearized plot of the equation. Accordingly, the Langmuir isotherm model is adequate to describe the phosphorus sorption process onto the prepared nanozinc oxide material. This result gives prediction that the sorption process of phosphorus ions onto the prepared ZnO nanorods takes place as monolayer sorption. The calculated maximum monolayer sorption capacity of phosphorus ions onto ZnO was 67 mg/g.

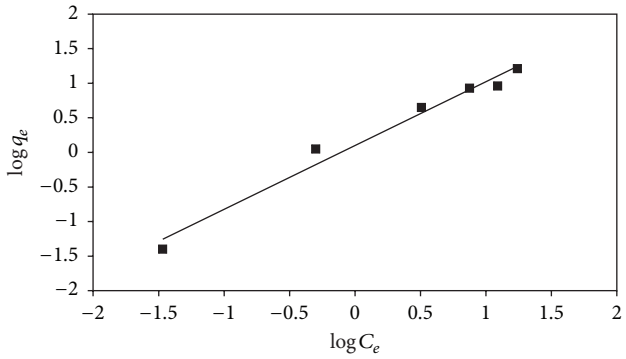

Figure 9: Freundlich equilibrium isotherm model for phosphorus ions sorption onto ZnO nanorods.

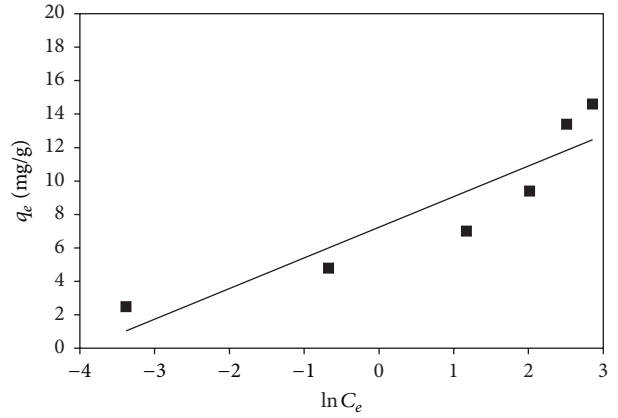

Figure 10: Temkin equilibrium isotherm model for phosphorus ions sorption onto ZnO nanorods.

3.3.2. Freundlich Model. Freundlich model shows the exponential distribution of active centers, characteristic of heterogeneous surfaces. Freundlich equation could be represented with the following linear one:

$$\ln q_e = \ln K_F + \left(\frac{1}{n_f}\right) \ln C_e, \tag{3}$$

where K_F and n represent adsorption capacity and intensity, respectively. K_F is an important constant which could be used as relative measure for adsorption efficiency. The magnitude of n shows an indication of the favorability of the adsorption process. Values of n larger than 1 show the favorable nature of adsorption.

The linear fits of phosphorus ions onto the synthesized nanozinc oxide were investigated in Figure 9. The validity of Freundlich model to describe the sorption process was acquired from the correlation coefficient value ($R^2 = 0.9782$) of the linear regression. It was evident that both Langmuir and Freundlich isotherm models are appropriate for describing the isothermal profiles of phosphorus sorption process onto the prepared zinc oxide nanopowder. These results indicated that the sorption process mainly occurs as monolayer and multilayers sorption process [26].

3.3.3. Temkin Model. By ignoring the extremely low and large value of concentrations, the model assumes that heat of adsorption (function of temperature) of all molecules in the layer would decrease linearly rather than logarithmically with coverage. This model could be expressed by the following linear equation [26]:

$$q_e = B_{\mathrm{T}} \ln K_{\mathrm{T}} + B_{\mathrm{T}} \ln C_e, \tag{4}$$

where K_{T} is Temkin isotherm equilibrium binding constant (L/g), corresponding to the maximum binding energy, and B_{T} is Temkin isotherm constant which is related to the heat of adsorption. Figure 10 gives the prediction that the phosphorus sorption process onto the zinc oxide nanopowder does not obey Temkin isotherm model where the equation linear fitting represents a comparatively lower value ($R^2 = 0.869$) compared with both Langmuir and Freundlich isotherm models. Finally, according to the equilibrium isotherm modeling results, the mechanism of phosphorus sorption process onto the prepared nano-ZnO mainly occurred through the physicosorption attraction of phosphorus ions onto the prepared ZnO nanorods; the nanorod morphology of prepared zinc oxide may enhance the physicosorption process compared with the nanoparticle morphological structure regarding its comparatively high surface area [27].

3.4. Kinetic Models for Phosphorus Sorption. Kinetic studies are important since they are not only providing valuable insights into the reaction pathways, but also describing the solute uptake rate which in turn controls the residence time of sorbate at the solid-liquid interface. In this respect, pseudo first-order, pseudo second-order, and intraparticle diffusion kinetic models were examined to describe the kinetics of phosphorus sorption onto prepared ZnO nanorods [27].

3.4.1. Pseudo First- and Second-Order Models. In order to find the order of phosphorus kinetic sorption, the investigated Lagergren and pseudo second-order equations were compared and their results were plotted in Figures 11 and 12 according to the following equations:

$$\log\left(q_e - q_t\right) = \log\left(q_e\right) - \left(\frac{k_1}{2.303}\right) t,$$
$$\left(\frac{t}{q_t}\right) = \left(\frac{1}{k_2 {q_e}^2}\right) + \left(\frac{1}{q_e}\right) t, \tag{5}$$

where q_e is the amount of phosphorus adsorbed at equilibrium (mg/g), q_t is the amount of phosphorus adsorbed at time t (mg/g), and k_1, k_2 are the rate constants of the pseudo first- and second-order kinetic sorption models, respectively (g/mg/h).

The calculated sorption capacity from the two equations and the linearization coefficients (R^2) were tabulated in Table 1. Based on the linearization coefficients, it was clear that the phosphorus sorption process follows the pseudo first-order model. Moreover, the calculated sorption capacities at the different studied phosphorus concentrations from the

Table 1: Estimated pseudo first- and second-order kinetic models parameters for phosphorus sorption onto ZnO nanorods.

Kinetic model	(q_e) exp (mg/g)	Pseudo first-order			Pseudo second-order		
Nitrate concentration (mg/L)		(q_e) cal (mg/g)	K_1 (min^{-1})	R^2	(q_e) cal (mg/g)	K_2 (g/mg min)	R^2
1	0.193	0.19	−0.052	0.998	0.34	0.089	0.97
10	1.89	1.88	−0.0053	0.987	2.56	0.018	0.95
25	4.35	4.3	−0.0053	0.99	5.87	0.0079	0.94
50	8.5	8.9	−0.006	0.99	11.67	0.0041	0.92
75	12.54	12.9	−0.076	0.99	22.98	0.00114	0.91
100	16.25	17.1	0.078	0.97	25.2	0.0012	0.90

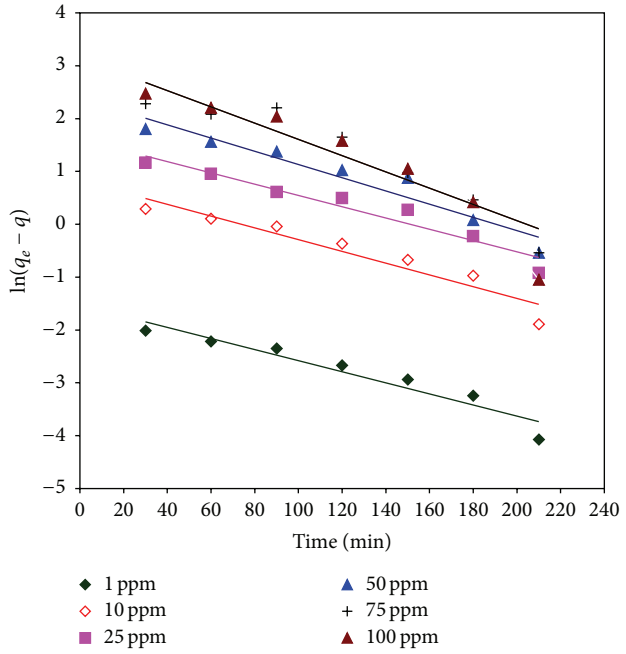

Figure 11: Pseudo first-order kinetic model for phosphorus ions sorption onto ZnO nanorods.

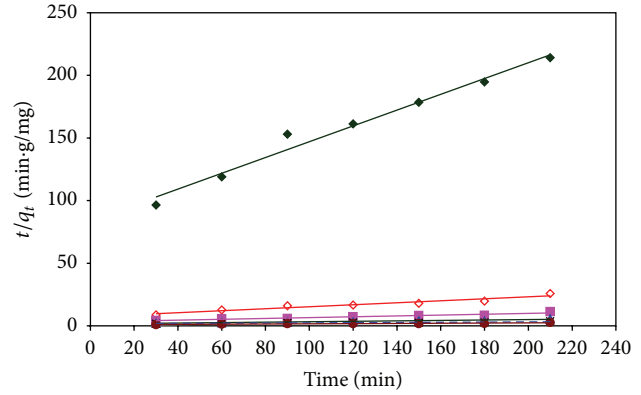

Figure 12: Pseudo second-order kinetic model for phosphorus ions sorption onto ZnO nanorods.

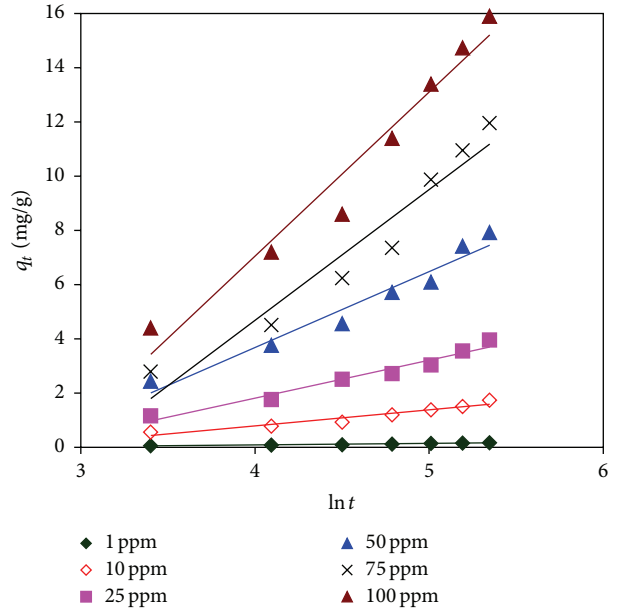

Figure 13: Intraparticle diffusion model for phosphorus ions sorption onto ZnO nanorods.

pseudo first-order model are close to the experimental capacities compared to that calculated from the pseudo second-order model. Accordingly, the kinetics of phosphorus sorption process onto the prepared ZnO follows the pseudo first-order model [28].

3.4.2. Intraparticle Diffusion Model. Weber and Morris found that, in many adsorption systems, the intraparticle diffusion resistance may affect the sorption process and the solute uptake varies almost proportionally with $t^{1/2}$ rather than the contact time t according to

$$q_t = K_i t^{0.5}, \quad (6)$$

where q_t is the sorption capacity at time t (mg/g/l) and k_i is the intraparticle diffusion rate constant, mg/g·min$^{-0.5}$.

As an attempt to describe the mechanism of phosphorus sorption onto the prepared zinc oxide, Figure 13 shows that the intraparticle diffusion model was adopted to describe the mechanism of the adsorption process. The results showed that the plots presented a multilinearity which indicated that two or more steps occurred in the process. R^2 values for this diffusion model were between 0.978 and 0.997, suggesting that the sorption process can be followed by an intraparticle

diffusion model. It can be also observed that the plots did not pass through the origin; this was indicative of some degree of boundary layer control and this further showed that the intraparticle diffusion was not the only rate-limiting step, but other processes might control the rate of phosphorus sorption process onto the prepared ZnO nanorods [29].

4. Conclusions

ZnO nanorods were successfully prepared using a simple ultrasonic technique in the presence of stabilizing agent. The crystalline and morphological structures of the prepared material were identified using SEM, TEM, and XRD, respectively. The feasibility of phosphorus ion removal onto the prepared material was tested using batch technique. The improvement in solution pH has negative effect on the phosphorus ion treatment process. However, the increment in contact time increases the treatment process. The equilibrium of phosphorus sorption process onto the prepared ZnO was described using Langmuir and Freundlich isotherm models. The kinetics of phosphorus sorption process follows the pseudo first-order model. The prepared ZnO nanorods were identified as good sorption material for both anions and cations.

Competing Interests

The authors declare that they have no competing interests.

Acknowledgments

This work was supported by the Egyptian Science and Technology Development Fund (STDF) (Grant no. 10763).

References

[1] H. Shokry Hassan, M. F. Elkady, A. H. El-Shazly, and H. S. Bamufleh, "Formulation of synthesized zinc oxide nanopowder into hybrid beads for dye separation," *Journal of Nanomaterials*, vol. 2014, Article ID 967492, 14 pages, 2014.

[2] H. Shokry Hassan, A. B. Kashyout, I. Morsi, A. A. A. Nasser, and A. Raafat, "Fabrication and characterization of gas sensor micro-arrays," *Sensing and Bio-Sensing Research*, vol. 1, pp. 34–40, 2014.

[3] X. Qu, P. J. J. Alvarez, and Q. Li, "Applications of nanotechnology in water and wastewater treatment," *Water Research*, vol. 47, no. 12, pp. 3931–3946, 2013.

[4] T.-T. Miao, D.-X. Sun, Y.-R. Guo et al., "Low temperature precipitation synthesis of flower-like ZnO with lignin amine and its optical properties," *Nanoscale Research Letters*, vol. 8, no. 1, pp. 431–439, 2013.

[5] M. F. Elkady and H. S. Hassan, "Equilibrium and dynamic profiles of azo dye sorption onto innovative nano-zinc oxide biocomposite," *Current Nanoscience*, vol. 11, no. 6, pp. 805–814, 2015.

[6] A. Askarinejad, M. A. Alavi, and A. Morsali, "Sonochemically assisted synthesis of ZnO nanoparticles: a novel direct method," *Iranian Journal of Chemistry and Chemical Engineering*, vol. 30, no. 3, pp. 75–81, 2011.

[7] M. F. Elkady, H. S. Hassan, E. E. Hafez, and A. Fouad, "Construction of zinc oxide into different morphological structures to be utilized as antimicrobial agent against multidrug resistant bacteria," *Bioinorganic Chemistry and Applications*, vol. 2015, Article ID 536854, 20 pages, 2015.

[8] B. Saha, S. Chakraborty, and G. Das, "A mechanistic insight into enhanced and selective phosphate adsorption on a coated carboxylated surface," *Journal of Colloid and Interface Science*, vol. 331, no. 1, pp. 21–26, 2009.

[9] S. R. Carpenter, "Phosphorus control is critical to mitigating eutrophication," *Proceedings of the National Academy of Sciences of the United States of America*, vol. 105, no. 32, pp. 11039–11040, 2008.

[10] Y.-F. Lin, H.-W. Chen, Y.-C. Chen, and C.-S. Chiou, "Application of magnetite modified with polyacrylamide to adsorb phosphate in aqueous solution," *Journal of the Taiwan Institute of Chemical Engineers*, vol. 44, no. 1, pp. 45–51, 2013.

[11] Z. Q. Zhu, H. H. Zeng, Y. N. Zhu et al., "Kinetics and thermodynamic study of phosphate adsorption on the porous biomorph-genetic composite of α-Fe_2O_3/Fe_3O_4/C with eucalyptus wood microstructure," *Separation and Purification Technology*, vol. 117, pp. 124–130, 2013.

[12] G. Laliberté, P. Lessard, J. de la Noüe, and S. Sylvestre, "Effect of phosphorus addition on nutrient removal from wastewater with the cyanobacterium *Phormidium bohneri*," *Bioresource Technology*, vol. 59, no. 2-3, pp. 227–233, 1997.

[13] D. J. Ballantine and C. C. Tanner, "Substrate and filter materials to enhance phosphorus removal in constructed wetlands treating diffuse farm runoff: a review," *New Zealand Journal of Agricultural Research*, vol. 53, no. 1, pp. 71–95, 2010.

[14] C. Vohla, M. Kõiv, H. J. Bavor, F. Chazarenc, and Ü. Mander, "Filter materials for phosphorus removal from wastewater in treatment wetlands: a review," *Ecological Engineering*, vol. 37, no. 1, pp. 70–89, 2011.

[15] M. H. Entezari and T. Soltani, "Simultaneous removal of copper and lead ions from a binary solution by sono-sorption process," *Journal of Hazardous Materials*, vol. 160, no. 1, pp. 88–93, 2008.

[16] T. Almeelbi and A. Bezbaruah, "Aqueous phosphate removal using nanoscale zero-valent iron," *Journal of Nanoparticle Research*, vol. 14, article 900, 2012.

[17] W. I. Park, G. C. Yi, D. H. Kim, and S. W. Jung, "Metalorganic vapor-phase epitaxial growth of vertically well-aligned ZnO nanorods," *Applied Physics Letters*, vol. 80, pp. 4232–4241, 2002.

[18] J. Du, Z. Liu, Y. Huang et al., "Control of ZnO morphologies via surfactants assisted route in the subcritical water," *Journal of Crystal Growth*, vol. 280, no. 1-2, pp. 126–134, 2005.

[19] E. R. Shaaban, Y. A. M. Ismail, and H. S. Hassan, "Compositional dependence of the optical properties of amorphous Se 80 - XTe20Bix thin films using transmittance and reflectance measurements," *Journal of Non-Crystalline Solids*, vol. 376, pp. 61–67, 2013.

[20] Y.-J. Tu, C.-F. You, C.-K. Chang, and M.-H. Chen, "Application of magnetic nano-particles for phosphorus removal/recovery in aqueous solution," *Journal of the Taiwan Institute of Chemical Engineers*, vol. 46, pp. 148–154, 2015.

[21] A. Akyol, H. C. Yatmaz, and M. Bayramoglu, "Photocatalytic decolorization of Remazol Red RR in aqueous ZnO suspensions," *Applied Catalysis B: Environmental*, vol. 54, no. 1, pp. 19–24, 2004.

[22] F. M. Omar, H. A. Aziz, and S. Stoll, "Aggregation and disaggregation of ZnO nanoparticles: influence of pH and adsorption of

Suwannee River humic acid," *Science of the Total Environment*, vol. 468, pp. 195–201, 2014.

[23] M. F. Elkady, E. M. El-Sayed, H. A. Farag, and A. A. Zaatout, "Assessment of novel synthetized nanozirconium tungstovanadate as cation exchanger for lead ion decontamination," *Journal of Nanomaterials*, vol. 2014, Article ID 149312, 11 pages, 2014.

[24] B. Alyüz and S. Veli, "Kinetics and equilibrium studies for the removal of nickel and zinc from aqueous solutions by ion exchange resins," *Journal of Hazardous Materials*, vol. 167, no. 1–3, pp. 482–488, 2009.

[25] T. Giang and P. Sreearunothai, "Magnetic particles for phosphorus adsorption in simulated phosphate solution," in *Proceedings of the 4th International Conference on Informatics, Environment, Energy and Applications (IEEA '15)*, vol. 82, pp. 144–148, 2015.

[26] Y. Saddeek, H. Shokry Hassan, and G. Abd Elfadeel, "Fabrication and analysis of new bismuth borate glasses containing cement kiln dust," *Journal of Non-Crystalline Solids*, vol. 403, pp. 47–52, 2014.

[27] M. F. Elkady, H. Shokry Hassan, and E. M. El-Sayed, "Basic violet decolourization using alginate immobilized nanozirconium tungestovanadate matrix as cation exchanger," *Journal of Chemistry*, vol. 2015, Article ID 385741, 10 pages, 2015.

[28] M. El-Aassar, M. El-Kady, H. S. Hassan, and S. S. Al-Deyab, "Synthesis and characterization of surface modified electrospun poly (acrylonitrile-co-styrene) nanofibers for dye decolorization," *Journal of the Taiwan Institute of Chemical Engineers*, vol. 58, pp. 274–282, 2016.

[29] M. F. Elkady and H. S. Hassan, "Invention of hollow zirconium tungesto-vanadate at nanotube morphological structure for radionuclides and heavy metal pollutants decontamination from aqueous solutions," *Nanoscale Research Letters*, vol. 10, no. 1, p. 474, 2015.